Journal of the Korean Society of Remote Sensing, Vol.16, No.2, 2000, pp.117~133

Sea Level Variations at Kerguelen Island in the South Indian Ocean by the Satellite Data(ARGOS) and Meteorological Data(METEO)

Hong-Joo Yoon

Dept. of Ocean Engineering, Division of Ocean System, Yosu National University

Abstract : We studied the sea level variations at Kerguelen island in the South Indian Ocean with ARGOS data and meteorological data during about 1 year(May 1993~April 1994) through using filter, spectral analysis, coherency and phase, and found characteristics for the two oceanic signal levels(detided oceanic signal level, $h_{detided}$ and seasonal oceanic level, $h_{corr.ib}$). The forms of atmospheric pressure variations are good agreed to between ARGOS data and meteorological data in the observed periods. This Kerguelen area shows the inflow of an air temperature(gain of a radiant heat) into the sea water and the stagnation of high atmospheric pressure bands in summer, and the outflow of a sea water temperature(loss of sensible and latent heat) toward the atmosphere and the stagnation of low atmospheric pressure bands in winter. The seasonal difference of sea level between summer and winter is about 1.6cm. Both the detided oceanic signal level($h_{detided}$) variation and the inverted barometer level(h_{ib}) variation have a strong correlation for T>1day period bands. The characteristics of $h_{detided}$ variation are not decided by the influence of any meteorological distributions (atmospheric pressure), but the influence of other factors(bottom water temperature) for T>2days periods bands. $h_{corr.ib}$ plays a very important role of sea level variation in the observed periods (especially T>about 180days period bands).

Key Words : Sea Level Variations, Inverted Barometer Variations

1. Introduction

Altimetric radar satellite in space provides measurements of the exact shape of the sea's surface and give an image not only of the seafloor's topography but also of the earth's interior. They can thus help to give a better understanding of the planet's internal dynamics. In the course of history of oceanography, the above results give also very important meaning in this field. That is to say, there are most recently the two scientific programs in relation to the utilization of satellite altimetry. The spatial missions of ERS1, Topex/Poseidon and Jason are good exemples. Especially altimetric data is utilized to understand many oceanic phenomena; for example, there are the investigations of both Tropical Ocean and Global Atmosphere(TOGA),

Received 10 March 2000; Accepted 25 April 2000.

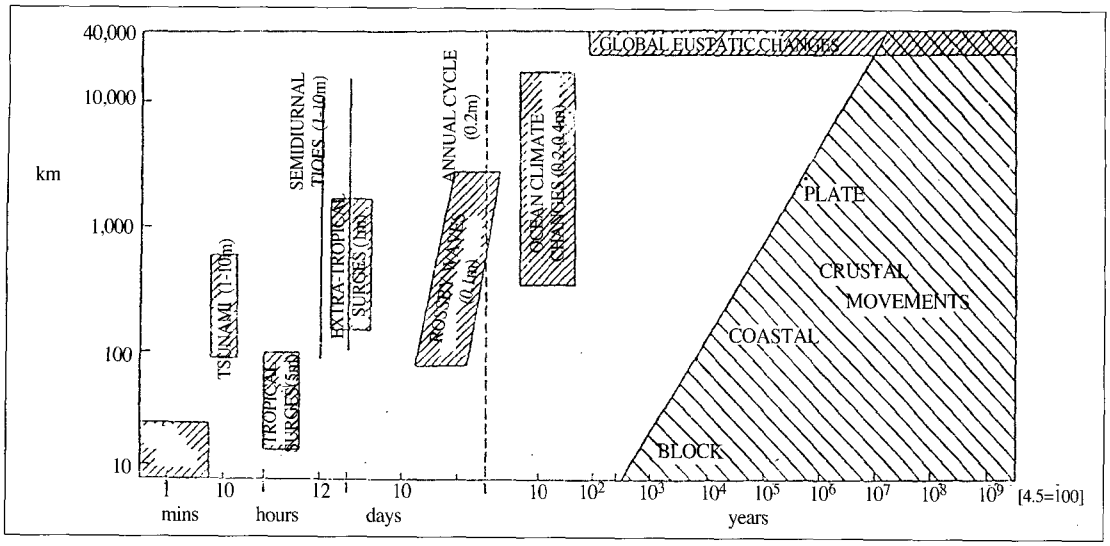

Fig. 1. Space-time relationship of sea level variations(by D. T. Pugh, 1990).

Tropical Atmosphere Ocean(TAO) and World Ocean Circulation Experiment(WOCE). These studies put emphasis on a more improvement of our knowledge for the hydrodynamic phenomena and on a more comprehension of an important role of their phenomena for the evolution of climate and global environments. The utilization of altimetry gives a global and repeated information for the study of basic parameters of sea level variations.

Sea level variation with the lapse of time shows the spatial and temporal scales in the ocean. This presents many various phenomena with hourly, daily, seasonal, annual and centurial, and the range from 10km to several 1000km(Fig. 1). A regular tidal phenomena, a remarkable and frequent upwelling according to the meteorological distributions and a wave due to a typhoon in small-scale, a wind and pressure in relation to circulation of the ocean in meso-scales, a wave which is occurring to extend over all the space in sea level variation, a phenomena of El Nino in connection with the evolution of climate in the annual sea level variation of water temperature (the steric variation) and of water volume(the eustatic variation) due to a freezing or melting of continetal glaciers in sea level variation of the long term, and a geometric variation of the basin of ocean in sea level variation of the very long term. Several sea level variation due to various phenomena as mentioned above becomes oceanic signal levels which have directly or indirectly an influence on sea level variation in the oceans(Table 1).

A striking climatological characteristic is occurred at Kerguelen island in the South Indian Ocean and a huge continental Self is located in the northern area of this island(Fig. 2). This area presents a Sea Surface Temperature(SST) of minus anomalies, a high heat losses of $-200W/m^2$ in the Austral Winter, and a wind stress and its curl of maximal values(Taljaard and Von Loon, 1984). On the oceanic environments of this area, several hydrological and dynamical studies had carried out in detail by Park et al.(1992, 1993).

The essential point of our study gains a better

Table 1. Various oceanic signal levels in sea-level variations

Signal	Amplitude	Periods
Tides	100-200cm	12-24 hours, month, year, 19-yrs day-week
Inverted bermeter effects	1-10cm (−1.01 cm/mbar)	
Effects of winds		
• Wave due to tempest	10-100cm	2-10 days
• Coastal upwelling	10-20cm	2-10 days
• Geostrophic current	slope < 10-5	>2π / f: interannual
- Large scale	1m / 100km	interannual
- Meseo scale	10cm / ≈ 100km	10-100 days
Seasonal effects		
• modulation of metelogicaleffects	40cm	annual - pluriannual
• Steric change	1-10cm	
Interannual effects		
• El Nino	10-50cm	
Eustatic Variation Steric variation	mm/year	very low frequency

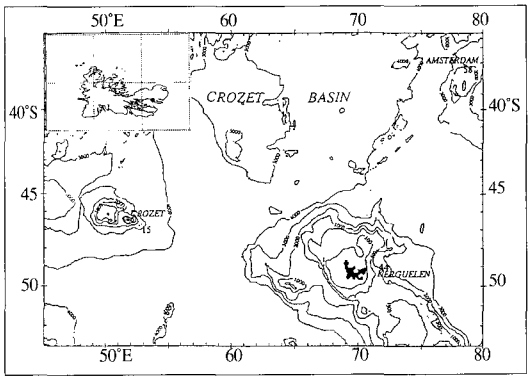

Fig. 2. Observation location of Port-Aux-Francais(70°14'E, 49°21'S) at Kerguelen island in the South Indian Ocean by METEO FRANCE.

understanding on characteristics both of detided oceanic signal level($h_{detided}$) and of seasonal oceanic signal($h_{corr.ib}$) among oceanic signal levels that contribute to sea level variations in this area.

2. Oceanic signal levels

The absolute sea level which is measured from the reference of geodetic surface gives generally expression to the sum of various kinds of oceanic signal levels as follows(Chelton and Enfield, 1986);

$$h_{sl} = h_t + h_p + h_w + h_e + h_s + h_c + h_g + \gamma \quad (1)$$

where, h_{sl} is sea level, ht is oceanic signal level by tidal influence(the high frequency tides), h_p is oceanic signal level by atmospheric pressure (inverted barometer effects; −1.01cm/mbar, $h_{ib} = h_p - \overline{h_p}$), h_w is oceanic signal level by winds(mainly the storm), he is oceanic signal level by eustatic changes(the global variation of water volume due to glaciers and oceanic basins), h_s is oceanic signal level by steric changes(the cause of changes of the sea water temperature and the salinity), h_c is oceanic signal level by circulation of the ocean(the origin of dynamic effects), h_g is oceanic signal level by coastal subsidence or tectonic effects from the geological motion and γ is oceanic signal level by human activites(the residual oceanic signal level for anthropogenic effects), respectively.

Seasonal oceanic signal level by steric changes is occurred by the expansion and contraction of water volume in the upper part of seasonal thermocline due to the variations of water flux or heat, but seasonal oceanic signal level by wind stress due to the horizontal and vertical movements(the Ekman flux and pumping) can be

neglected in seasonal time scales(Gill and Miller, 1973). Also h_e, h_g and γ which are a global and centurial oceanic signal level variation do not nearly contribute to as seasonal oceanic signal level variation in seasonal time scales. But the contribution of h_c(oceanic signal level due to various currents in relation to the circulation of ocean in a Neighborhood Seas) could not be ignored in this observed station because this station is nearby located in the area which is being formed the Polar Front with the Antarctic Surface water. On the other hand, considering a geological situation of this station(see Fig. 2), it should be thought that oceanic signal level variation by currents is greatly defectived in this station. Thus from various obvious facts of the above in our study, equation(1) can be simply reduced to

$$h_{sl} = h_t + h_{ib} + h_s \quad (2)$$

$$h_{detided} = h_{sl} - h_t \quad (3)$$

$$= h_{ib} + h_s \quad (4)$$

$$\text{with } h_{ib} = h_p - \overline{h_p} \quad (5)$$

also equation(3) and (4) can be again written

$$h_{corr.ib} = h_{detided} - h_{ib} \quad (6)$$

$$= h_s \quad (7)$$

where, $h_{detided}$ is detided oceanic signal level when h_t is only removed from h_{sl}, h_{ib} is inverted barometer level, that is say, this is anomaly of atmospheric pressure, and $h_{corr.ib}$ is seasonal oceanic signal level when h_t and h_p are removed from hsl, respectively.

3. Data and Processing Method

Atmospheric and bottom pressure, bottom water temperature(ARGOS data with dt = 1hour at ARGOS satation; 70°13'E and 49°20'S, Fig. 3), and atmospheric pressure and winds(METEO

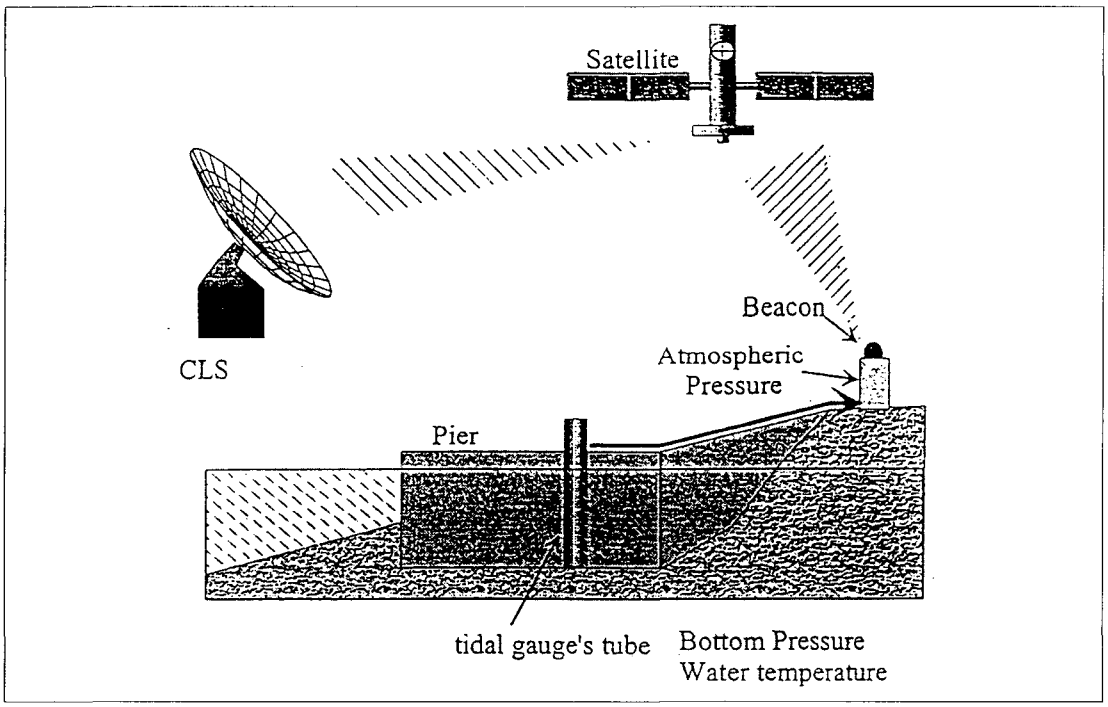

Fig. 3. Permanent sea level observation(●, 70°13'E, 49°20'S) by ARGOS system.

FRANCE data with dt = 3hours at Port Aux Francais station; 70°14'E and 49°21'S) were used in our study during May 1993~April 1994.

Fig. 4 shows a brevity schema for data processing method. Fig. 5 presents sea level variation with the time changes. If bottom pressure($P_{(t)b}$) depends on atmospheric pressure ($P_{(t)a}$) and its relationship is constant during all the observed times, a good equation can be leaded by using hydrostatic equation.

$$P_{(t)b} = \rho g(H+h_{(t)sl}) + P_{(t)a} \quad (8)$$

where, ρ is density in sea water, g is gravity, H is mean sea level and $h_{(t)sl}$ is sea level variation with the lapse of time, respectively. If mean value of $h_{(t)sl}$ is zero($h_{(t)sl} = 0$), then mean sea level can be obtained from equation(8).

$$H = \frac{P_{(t)b} - P_{(t)a}}{\rho g} \quad (9)$$

both the sea level variation with the time changes on the basis of mean sea level and the oceanic signal level by inverted barometer effects can be calculated as follows, respectively;

$$h_{(t)sl} = \frac{P_{(t)b} - P_{(t)a}}{rg} - H \quad (10)$$

$$= \frac{P_{(t)b} - P_{(t)a}}{\rho g} - \frac{P_{(t)b} - P_{(t)a}}{\rho g} \quad (11)$$

$$= \frac{dP_{(t)b} - dP_{(t)a}}{\rho g} \quad (12)$$

$$h_{(t)ib} = -\frac{P_{(t)a} - \overline{P_{(t)a}}}{\rho g} \quad (13)$$

$$= -\frac{dP_{(t)a}}{\rho g} \quad (14)$$

with $dP_{(t)b} = P_{(t)b} - \overline{P_{(t)b}}$ (15)

$dP_{(t)a} = P_{(t)a} - \overline{P_{(t)a}}$ (16)

In order to determine the amplitude of tides at this station, tidal prediction model(Le provost C., 1981; Cartwright and Ray, 1990) had calculated through harmonic analysis which is

$$h_{(t)} = \sum_{i=1}^{n} f_i A_i \cos(\omega_i + (v_0 + u_i) + g_i) \quad (17)$$

n is the index number of harmonic constants, f_i is the relative nodal correction, u_i, is the nodal correction factor with 18.16, A_i is amplitude, ω_i is angular velocity, $(v_0 + u_i)$ is phase(the equilibrum argument)

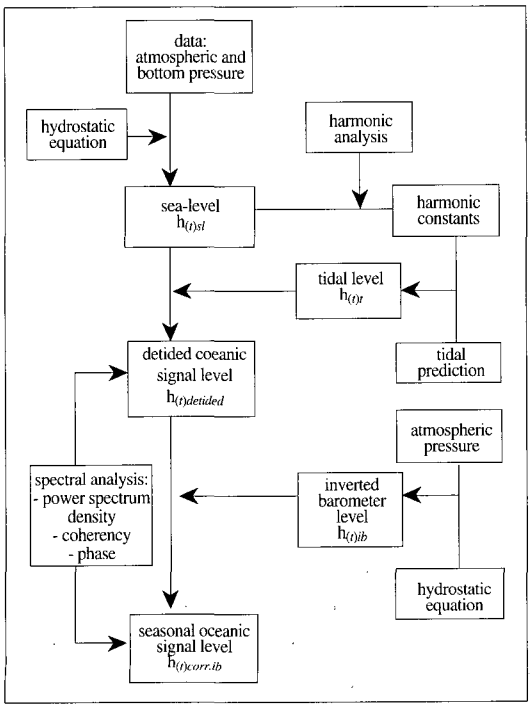

Fig. 4. Data processing method.

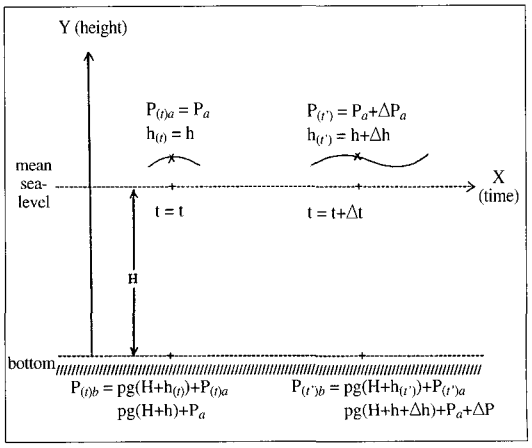

Fig. 5. Sea level variation with the time changes.

at Greenwich Merdian as t=0, and g_i is the difference of phase from Greenwich Merdian, respectively.

4. Results and Consideration

Their shapes for atmospheric pressure variations with the time changes are good agreed between satellite data(ARGOS) and meteorological data(METEO) during the observed periods (Fig. 6a). Where the differences of between ARGOS and METEO appears $dP = (P_{ARGOS} - P_{METEO})$, and dP does not show the parallel line as

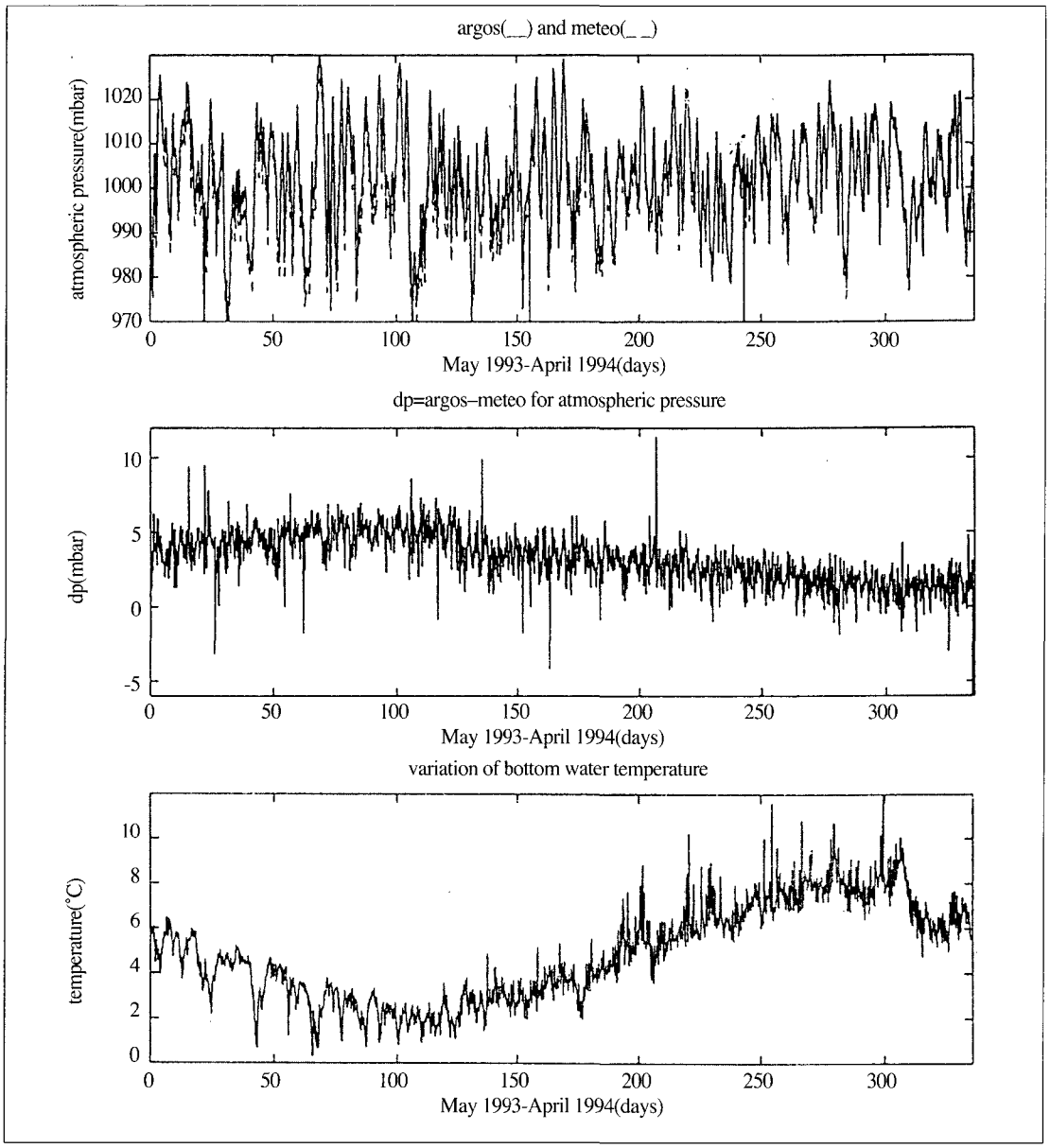

Fig. 6. Variations of (a) atmospheric pressure(–: ARGOS data, - -: METEO data), (b) deviations between ARGOS data and METEO data for atmospheric pressure and (c) bottom water temperature.

a constant form at the observed periods(Fig. 6b). Bottom Water Temperature(BWT) seasonally varies with a range of about 0~10℃(Fig. 6c).

Fig. 7a shows the regression equation(Y_{mbar} = −0.53 $X_{℃}$ + 5.8558) between BWT and dP, and here are the two groups on the basis of the mean values of both X=4.856℃ and Y=3.219mbar for all data in the observed periods. As comparing BWT and *dP* after using the low-pass filter(gaussian filter) with T= 3day-period cut-off, they represent completely a anti-correlation with the correlation coefficient of r=−0.8229(Fig. 7b). It could be devided by the

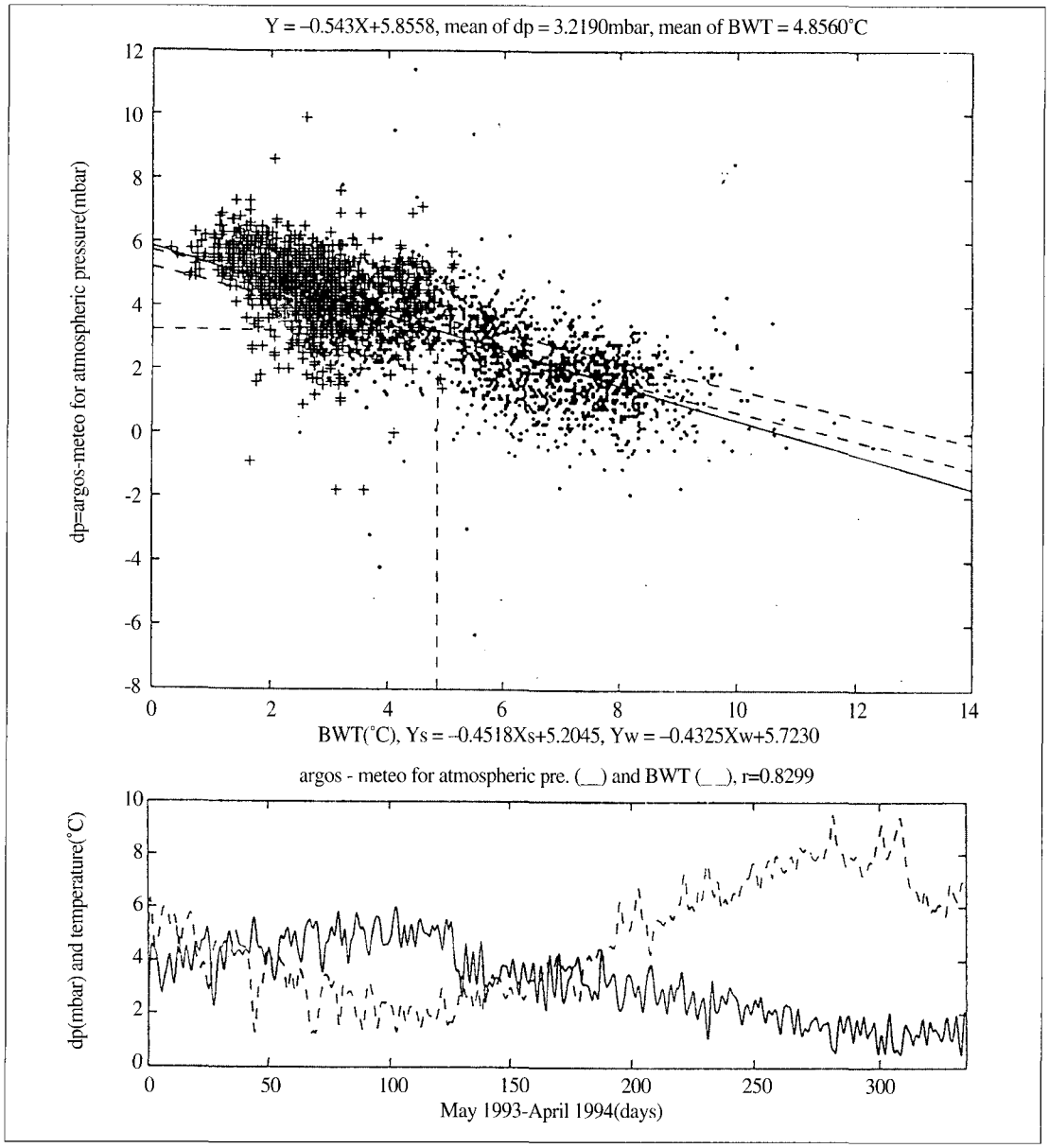

Fig. 7. In bottom water temperature and dP, (a) the regression equation and (b) the comparison after using the low-pass filter with a cut-off at 3 day period.

seasonal characteristics from the concentration as group 1 and group 2; group 1 represents the spring and summer in Southern Hemisphere (October~December 1993 and January~March 1994) and group 2 the autumn and winter in Southern Hemisphere(June~September 1993). Then two regression equationsfor both group 1 and group 2 are Y_{mbar} = −0.4518 $X_{°C}$ + 5.2045 in summer and Y_{mbar} = −0.4325 $X_{°C}$ + 5.7230 in winter, respectively.

Fig. 8 shows the mean values of every factor (atmospheric, bottom and dP pressure, and BWT for ARGOS and METEO) in all the observed periods, the spring and summer(group 1) and the autumn and winter(group 2), respectively. Firstly group 1 is 2.1 times larger in BWT and about

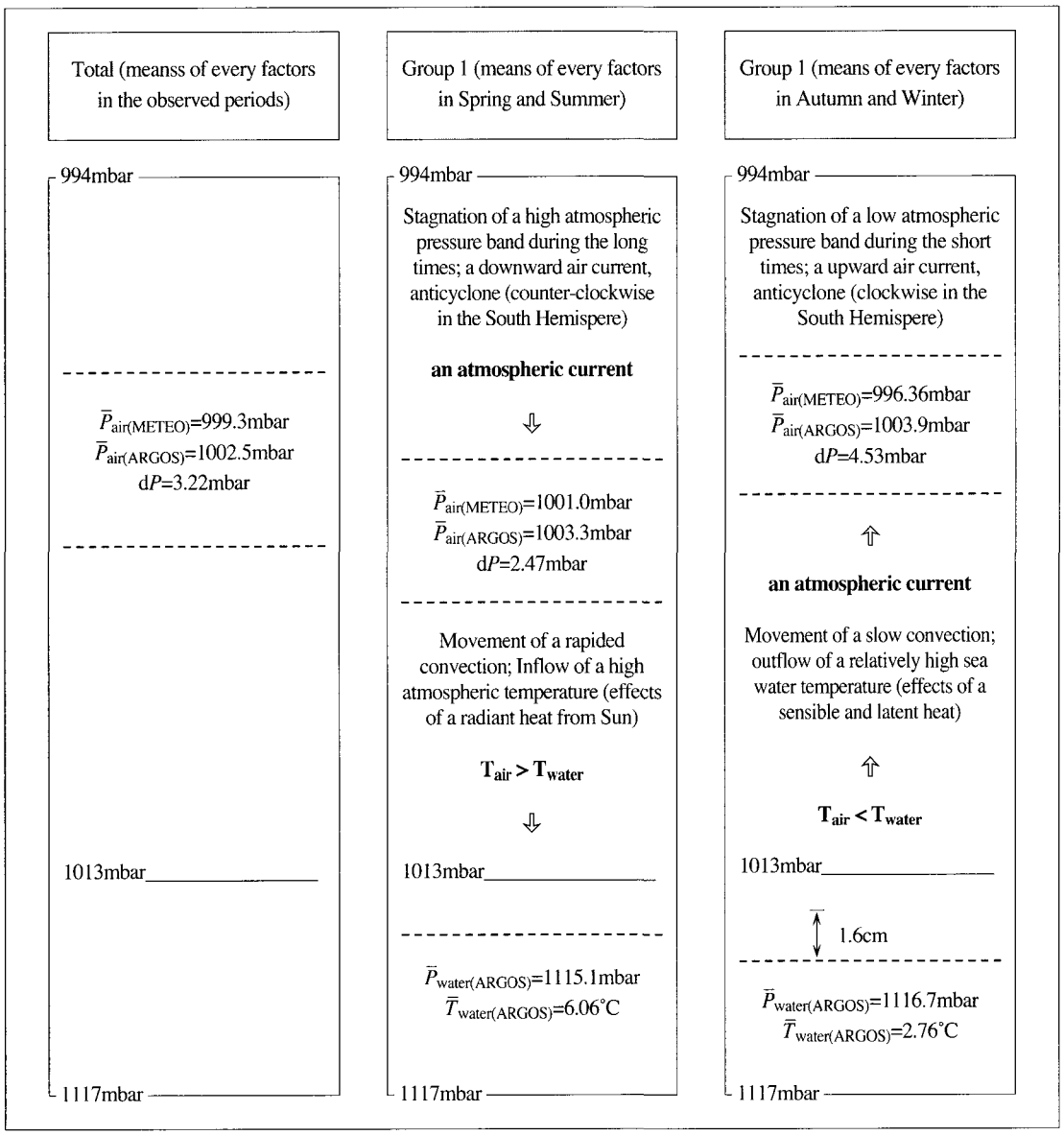

Fig. 8. Mean values for atmospheric, bottom and dP pressure, and BWT, respectively.

1.8times larger in Root Mean Square(RMS) against to group 2. It should be explained that a high atmospheric temperature which is increased by a radiant heat from Sun(in the spring and summer; group 1) inflows into sea water(movement of a rapid convection; $T_{air}>T_{water}$), and a relatively high sea water temperature comparing to a atmospheric temperature(in the autumn and winter; group 2) outflows from sea water (movement of a slow convection; $T_{air}<T_{water}$, effects of a sensible and latent heat losses). Secondly dP of group 2 is about 1.8times more than that of group 1, and RMS of the two group are nearly the same values. This should be considered on the meteorological characteristics that this Kerguelen area forms a stagnation of a low atmospheric pressure bands(a upward air or atmospheric current, cycle in the southern Hemisphere) during the short times(4 months in group 2), and a stagnation of high atmospheric pressure bands(a downward air current, anticyclone; counter-clockwise in the southern Hemisphere) during the long times(7 months in group 1). Finally the difference of sea level between group 1 and group is about 1.6cm.

Fig. 9 shows variations of (a) sea level, h_{sl}, (b) tidal level, h_t, (c) detided oceanic signal level, $h_{detided}=h_{sl}-h_t$, (d) inverted barometer level, $h_{ib}=h_p-\overline{h_p}$ and (e) seasonal oceanic signal level, $h_{corr.ib}=h_{detided}-h_{ib}$, respectively. Fig. 10 shows power spectrum density for (a) h_{sl}, (b) h_t, (c) $h_{detided}$ and (d) BWT. When setting on the basis of T=3days period, h_{sl} variation shows high values of energy in all the band and h_t variation very low values of energy in all the band except several stronger peaks of energy in T<3days period bands. Thus these results mean that tides(high frequency tides) do not greatly contribute to h_{sl} variation in the long periods as compared to $h_{detided}$ variation in the distribution of energy of all the period bands. So to speak, this should be explained that BWT with the seasonal and annual time scales contributes to h_{sl} variation in the long periods.

The above results show an important bearing on the relations of $h_{detided}$ to h_{ib}. Thus giving attention to both $h_{detided}$ and h_{ib}, this two oceanic signal levels appear a smilar form with the lapse of time. In order to know exactly periodicity or regulation of their relationship(Fig. 11), these two oceanic signal levels were filtered by gaussian's the low-pass filter method(T=3days period cut-off). We note that there is a strong correlation between $h_{detided}$ variations and h_{ib} variations with r=0.87. This means that oceanic signal level by inverted barometer effects is the most superior among all the oceanic signal levels for contributions of sea level variations.

As comparing with $h_{detided}$ and h_{ib} through spectral analysis, cm, coherency, γ^2 and phase, θ in Fig. 12. On spectral analysis, $h_{detided}$ appears sea level of about 4.8cm in T=about 10days period and about 5.6cm in T=about 180days period, and h_{ib} appears sea level of about 6.6cm in T=about 10days period, respectively(Fig. 12a). On coherency squared, these two levels($h_{detided}$ and h_{ib}) show a good relation with $r^2=0.46$(the confidence level is 95%) for T>1days period bands(Fig. 12b). On phase, the response of $h_{detided}$ to atmospheric forcing distributions is advanced than the response of h_{ib} response in the high frequency with T<2days period bands, but the response of $h_{detided}$ to atmospheric forcing distributions is slower than the response of h_{ib} in the low frequency variation with T>2days period bands(Fig. 12c). The above results mean that characteristics of $h_{detided}$ variation are decided not by the influence of any atmospheric forcing distributions(atmospheric pressure) but by the

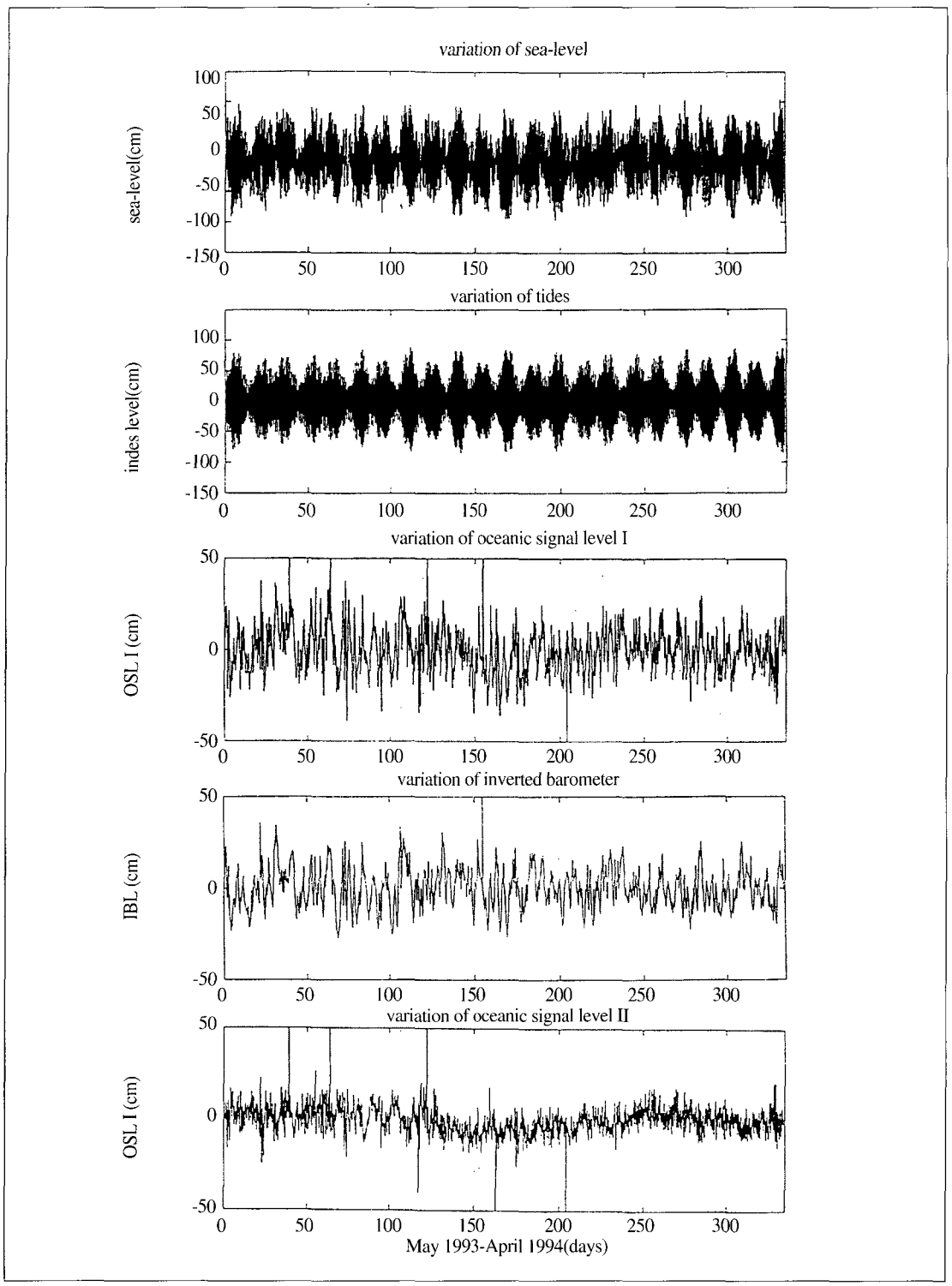

Fig. 9. Variations of (a) sea level, h_{sl}, (b) tidal level, h_t, (c) detided oceanic signal level, $h_{detided} = h_{sl} - h_t$, (d) inverted barometer level, $h_{ib} = h_p - \overline{h_p}$ and (e) seasonal oceanic signal level, $h_{corr.ib} = h_{detided} - h_{ib}$, respectively.

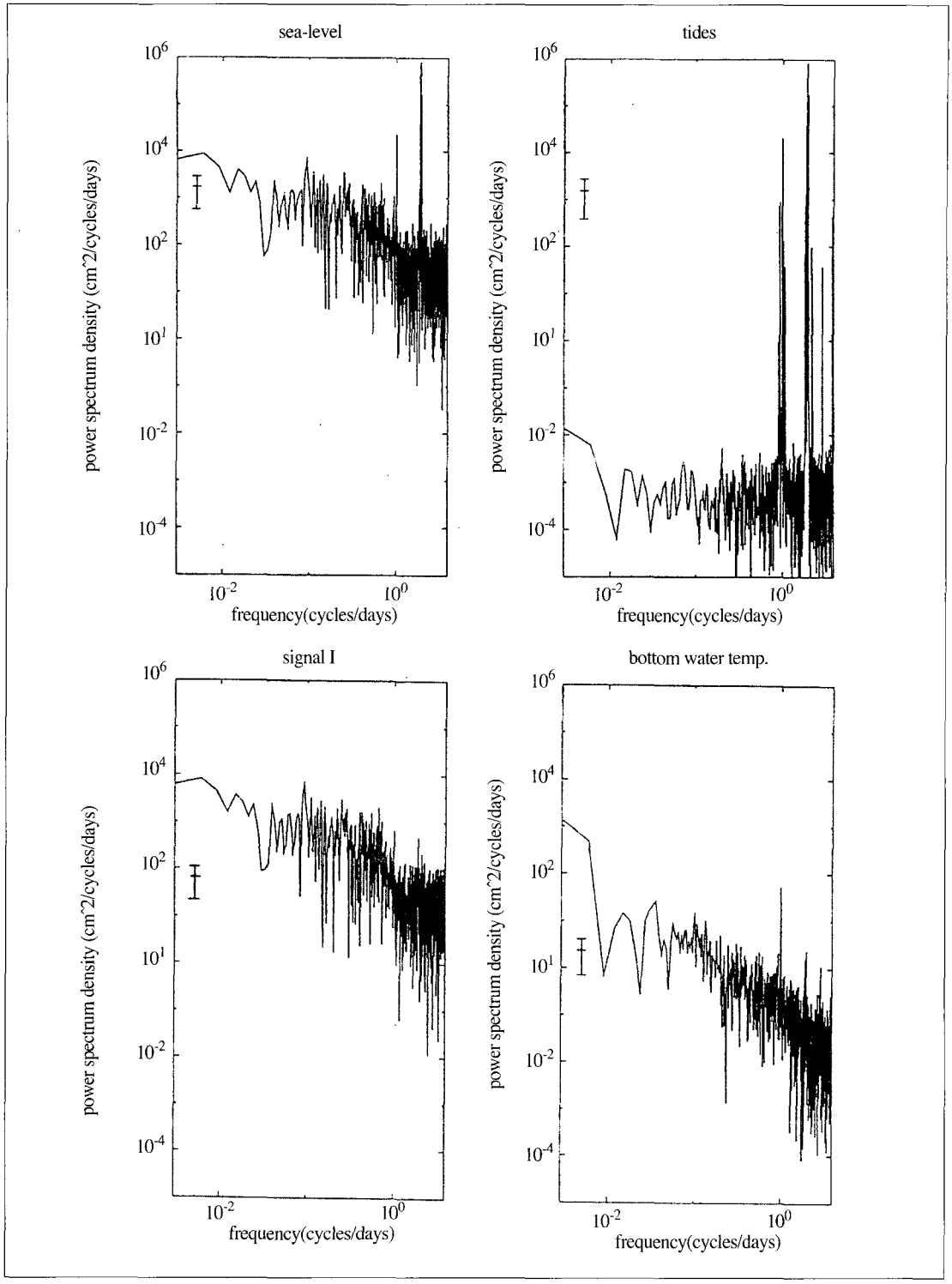

Fig. 10. Power spectrum density for (a) sea level, (b) tides, (c) detided oceanic signal and (d) bottom water temperature, respectively, the confidence intervals are 95%.

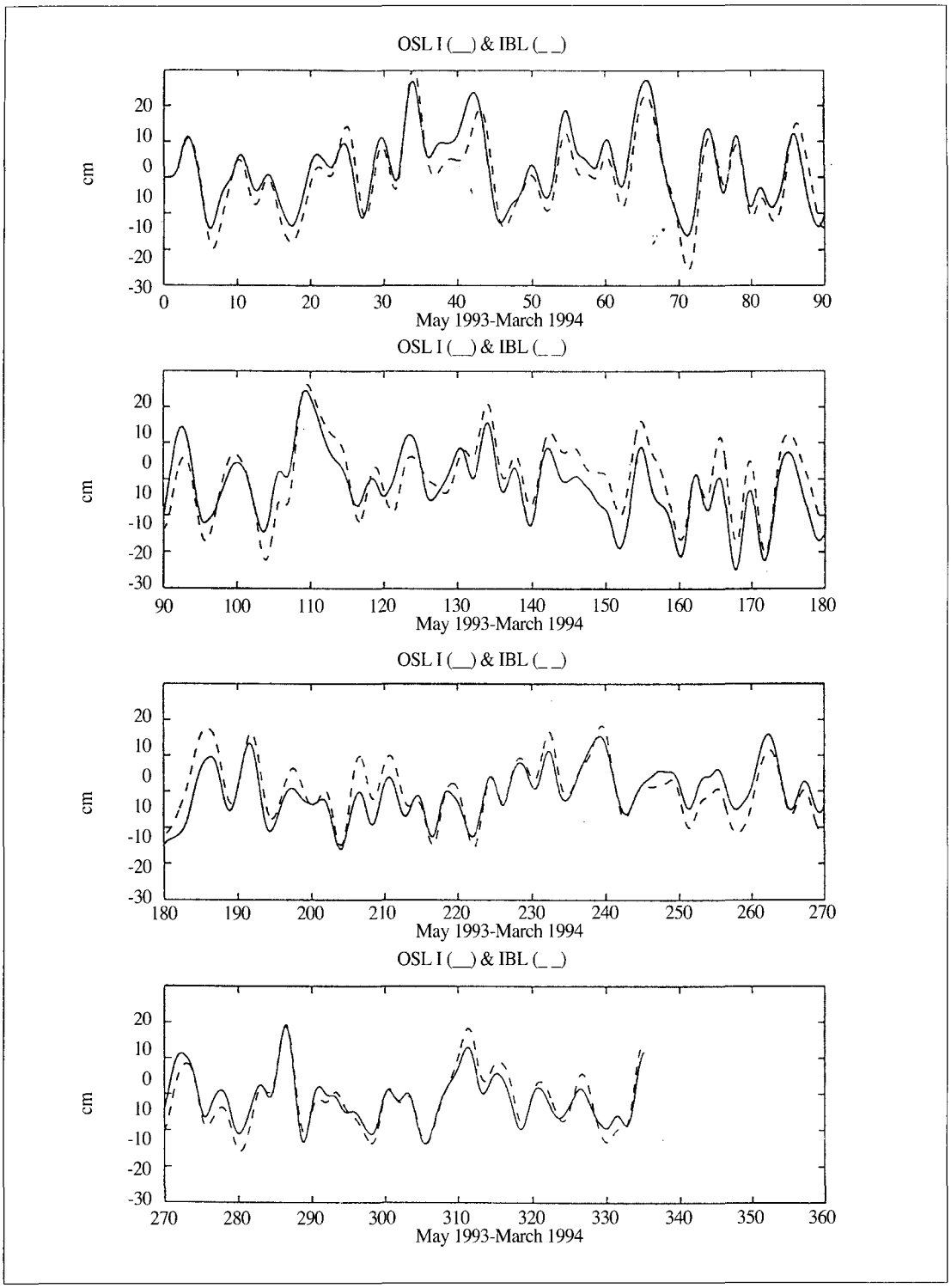

Fig. 11. Variations of detiede oceanic signal level(—) and inverted barometer level(– –) after low-pass filter(gaussian filter) with a cut-off 3 day period.

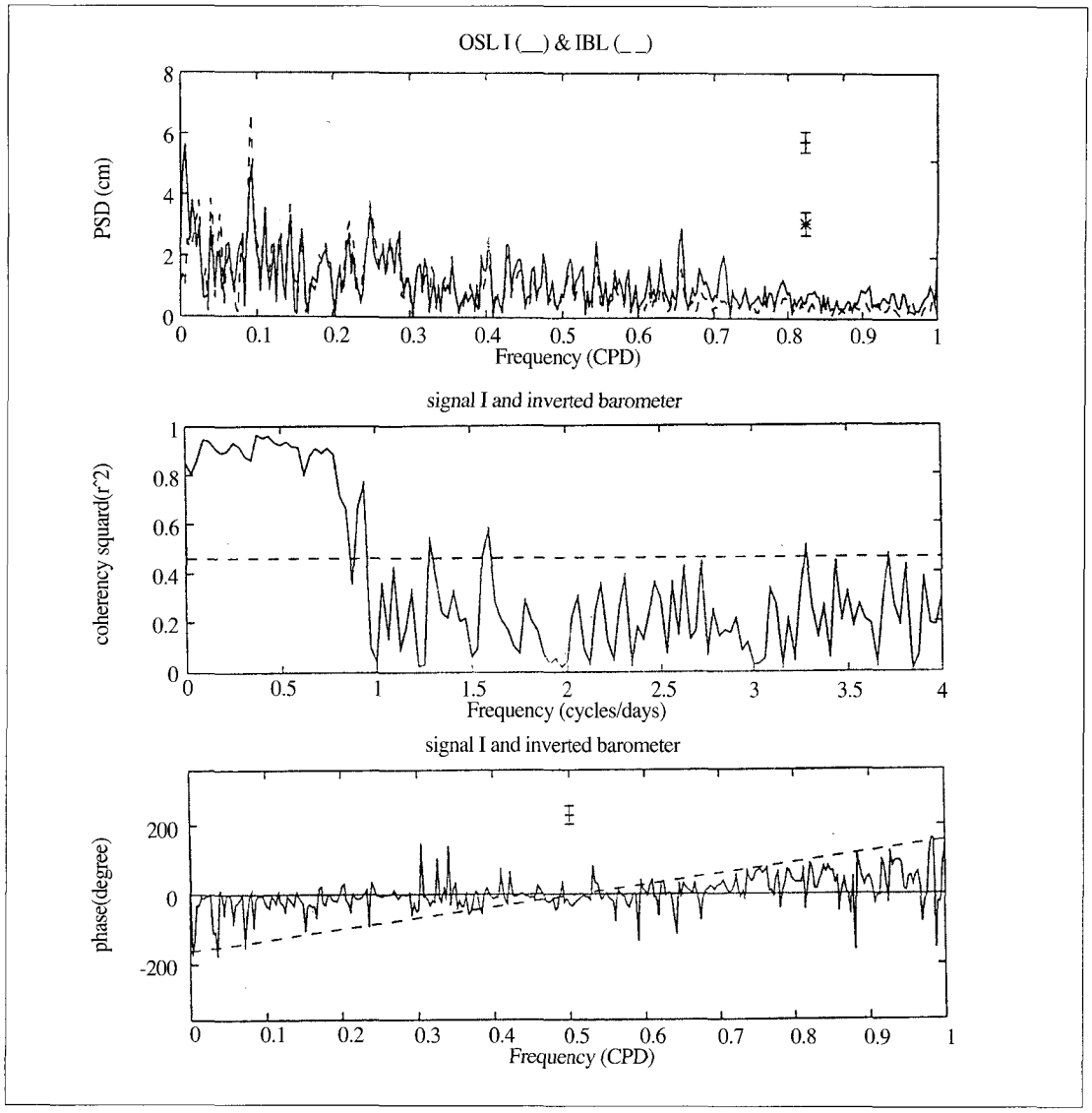

Fig. 12. Comparing with detided oceanic signal level and inverted barometer level through (a) spectral analysis, cm, (b) coherency squard, γ^2 and (c) phase, θ. Here, the confidence intervals are 95% and the confidence level is 0.46, respectively.

influence of other factors(BWT) in the turning point of T>2days period bands in the variations of long periods.

Sea level variations present usually a range of a distinct variation of about semi-annual or annual seasonal characteristics with amplitudes of 2~3cm at low latitudes and of about 10cm at high latitudes in monthly and annual time scales. Seasonal oceanic signal level, $h_{corr.ib}$, variations are basically caused by simutaneously seasonal modulation of meteorological effects and thermal structure of sea surface(warming up or cooling down by seasonal variations in sea surface). As thinking over $h_{corr.ib}$, seasonal oceanic signal level, there are a necessity to know their relationship between $h_{corr.ib}$ and BWT. Fig. 13a and 13b show

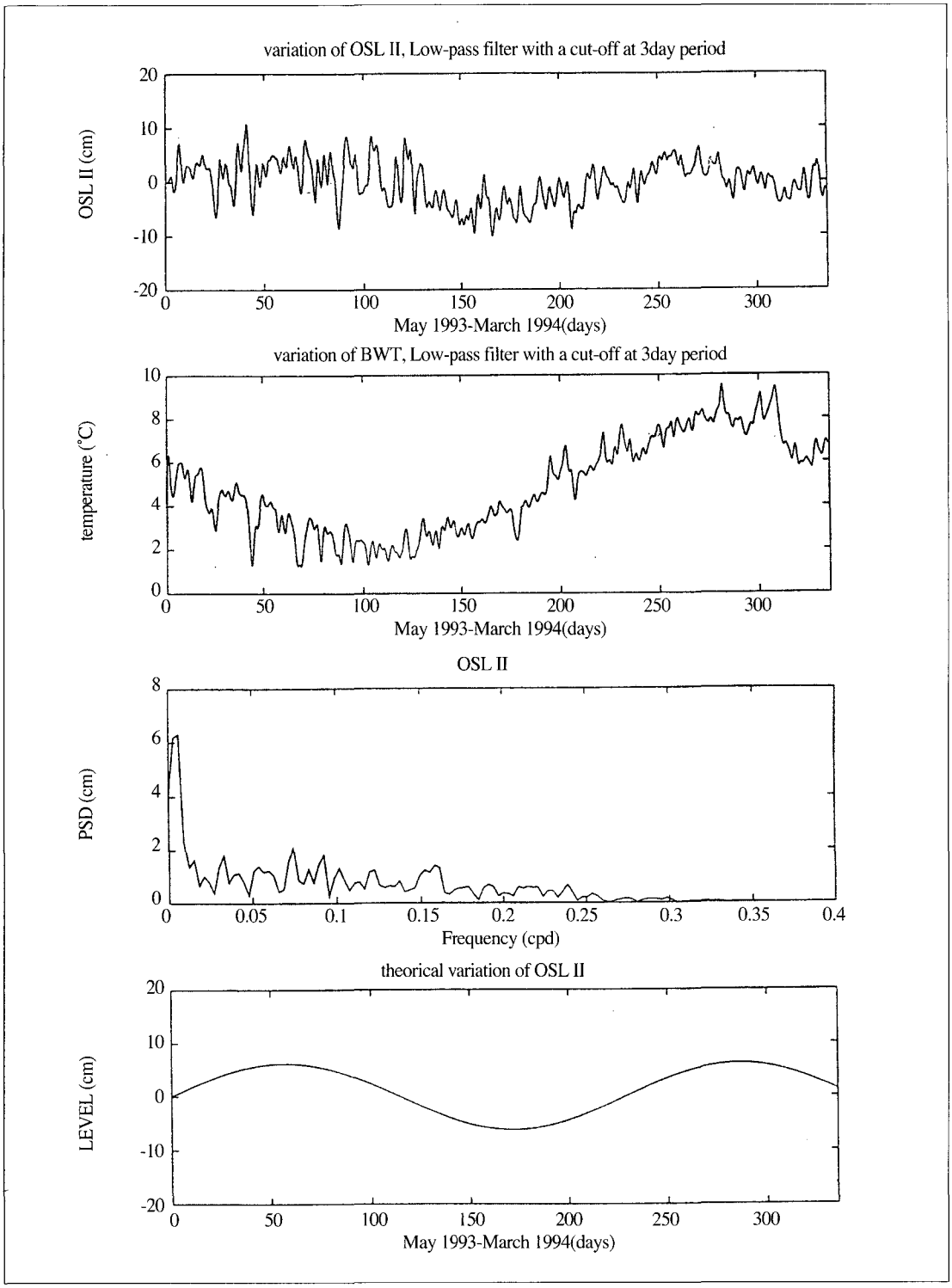

Fig. 13. Variations of (a) seasonal oceanic signal level and (b) bottom water temperature after low-pass filter with a cut-off 3 day period, (c) power spectrum density of seasonal oceanic signal level, and (d) theorical variations of seasonal oceanic signal level.

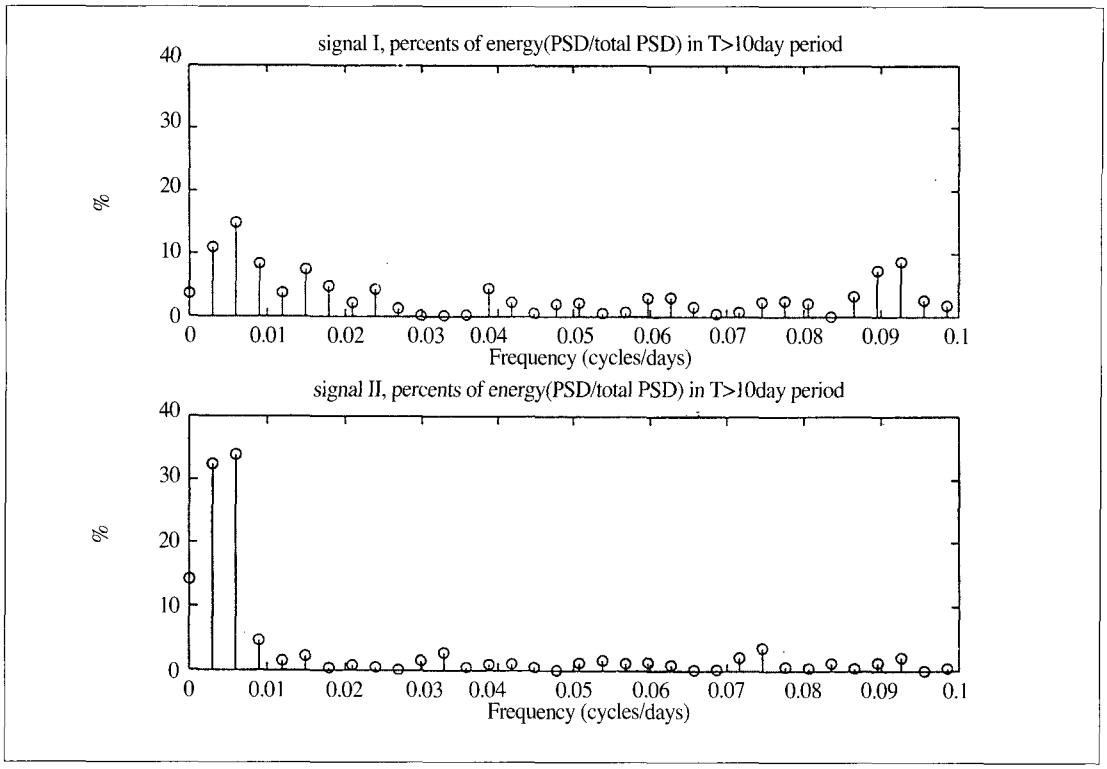

Fig. 14. Comparing with (a) detided oceanic signal level and (b) seasonal oceanic signal as energy percent in power spectrum density.

once more again the represented figure after low-pass filtering with a cut-off at 3day period for both $h_{corr.ib}$(Fig. 9e) and BWT(Fig. 6c), and Fig. 13c presents the power spectrum density of $h_{corr.ib}$ in T>3days period bands. Here, we can know that $h_{corr.ib}$ varies approximately with a form of sine function in relation to seasonal variations of BWT with a certain regulation during this observed periods, and that then $h_{corr.ib}$ has generally a high peak of energy in the long periods. that is say, it should be explained that seasonal oceanic signal level($h_{corr.ib} \cong 6.2 \sin(\frac{\pi}{2}t + \frac{\pi}{6}6)$, unit: cm) due to steric changes(the seasonal variation of BWT) is contributing to sea level variations in monthly and annual time scales(Fig. 13d).

Fig. 14 shows the energy percent(PSD/total PSD) in T>10days period bands for both $h_{detided}$ and $h_{corr.ib}$, then $h_{detided}$ and $h_{corr.ib}$ have about 12.3884cm and 7.4268cm for RMS, and about 30% and 80% for energy percent, respectively. This means that a contribution of $h_{corr.ib}$ is superior to that of $h_{detided}$ for sea level variations in T>100days period bands.

5. Conclusions

We obtained the several results from the two oceanic signal levels($h_{detided}$ and $h_{corr.ib}$) on sea level variations at Kerguelen island in the South India Ocean by using filter, power spectrum density, coherency and phase. Their spectral shapes for atmospheric pressure variations are good agreed with between ARGOS data and METEO data in

all the observed periods. Regression equation and correlation coefficient between BWT and dP is $Y_{mbar} = -0.53\ X_{^\circ C} + 5.8558$ and r=−0.8299 in the all periods, respectively. This Kerguelen area appears (a) firstly the inflow of a high atmospheric temperature to sea water(effects of a radiation heat by Sun) and the stagnation of a high atmospheric pressure bands during the long times in the spring and summer, and (b) secondly the outflow of a relatively high sea water temperature from sea water(effects of a sensible and latent heat losses) and the stagnation of low atmospheric pressure bands during the short times in the autumn and winter, respectively, and (c) finally the difference of sea level between spring-summer and autumn-winter is about 1.6cm.

Also we found an important characteristic for two oceanic signal levels(detided oceanic signal level, $h_{detided}$ and seasonal oceanic signal level, $h_{corr.ib}$) due to the meteorological effects(inverted barometer level, h_{ib}) and seasonal effects(bottom water temperature), respectively. There is strong correlation between $h_{detided}$ and h_{ib} for T>1day period bands in coherency, and characteristics of $h_{detided}$ variations are decided not by the influence of any atmospheric distributions (atmospheric pressure), but by the influence of other factors (bottom water temperature) for T>2days period band in phase. The theological variations of seasonal oceanic signal level($h_{corr.ib} \cong 6.2 \sin(\frac{\pi}{2}t + \frac{\pi}{6})$) due to steric changes(the seasonal variation of bottom water temperature) is contributing to sea level variations in the monthly and annual time scales. The signal level $h_{corr.ib}$ plays a very important role of the sea level variations of the long periods in comparison with $h_{detided}$ because $h_{corr.ib}$ has the high energy percent of 80%(PSD/total PSD) in T>10days period bands.

Both agricultural and industrial, human activities, cause the emission of ploy-atomatic molecules into the atmosphere. It is known that the green house effects cause a global warming. The augmentation of temperature brings about a global rise in mean sea level resulting from melting glaciers and polar ice caps and to the thermal expansion of sea water. Generally an upper limit of 60cm be estimated for the rise in global sea level by the end of the 21C(Welander, 1990), but this estimate is fraugt with large incertitudes. But whatever parameters contribute to sea level rise, our deep interests should be paid attention to sea level variations as a global warning for the Earth's environments.

Acknowledgemants

ARGOS data were provided by CLS-ARGOS/SAM and meteorological data were made available by the METEO FRANCE at Kerguelen island. Thanks Prof. C. Le Provost and Dr. J. M. Molines for discussion on this paper. This Study is supported by Yosu National University through Research Fund.

References

Cartwright, D. E. and R. D. Ray, 1990, Oceanic Tides from Geosat altimetry, J. of Geophysical Research, 95(3): pp. 3069-3090.

Chelton, D. B. and D. B. Enfield, 1986. Ocean signals in Tide Gauge Records, J. of Geophysical Research. 91(9): pp. 9081-9098.

Gill, A. E. and P. P. Miller, 1973. The theory of the seasonal variability in the ocean, Deep-sea Res., 20, pp. 141-177.

Koblinsky, C. J., P. gaspar, D. Loyerloet, 1992, The

future of Spaceborne Altimetry, ocean and climate change, Joint Oceanographic Institute, Washington, D. C., pp.75.

Le Provost C., 1981, A model of prediction of tidal elevation over the English Channel, Oceanol. Act. 4, 3.

Le Provost C., 1991, La meteorologi, VII Serie, No. 40, pp. 3-12.

Pugh, D. J., 1987, Tides, Surges and Mean Sea Level, Chichester, John Wily & Sons, Ltd, pp. 472.

Park, Y. H. and S. G. bernard, 1992, Sea level variability in the Crozet- Kerguelen-Amsterdam Area from Bottom Pressure and Geosat Altimetry, Geophysical Monography 69, IUGG Volume II, pp. 117-131.

Park, Y. H., Gamberoni and E. charriaud, 1993, frontal structure, water Masses, and Circulation in the Crozet basin, J. of Geophysical Res., 98(7): pp. 12361-12386.

Rabiner, L. R. and B. Gold, 1975, Theory and Application of Digital signal processing, Prentice-Hall, Englewood Cliffs, N. J..

Taljaard, H. A. and H. von Loon, 1984, Climate of the Indian Ocean South of 35°S, in Climate of the Oceans edited by H. von Loon, pp. 505-601, Elsevier Amsterdam, 1984.

Welander, P., 1990, Global sea level Change on the decimal to century time scales, Discussion of scientific problem in contex of NOAA's program 'Climate and Global Change', with recommendation, University of Washington, Seattle, pp. 35-49.